

Advanced InSb–Sb eutectic alloys with tailored interfaces for high thermoelectric efficiency

M.V. Kazimov^{1,3,4*}, G.B. Ibragimov^{1,3}, B.G. Ibragimov^{1,2}

¹The Ministry of Science and Education of the Republic of Azerbaijan, Institute of Physics, G. Javid ave 131, AZ1073 Baku

²Azerbaijani-French University, 183 Nizami street, Baku, Azerbaijan

³Baku State University, Az1148, Z. Khalilov str., 23, Baku, Azerbaijan

⁴Sumgait State University, Sumgait city, 43rd district, Baku street 1, AZ5008

*Corresponding author e-mail: mobilkazimov@gmail.com

Abstract. An InSb–Sb eutectic composite made by the Bridgman method has been analyzed using structural and differential scanning analysis, Raman scattering, and X-ray diffraction. It has been shown that needle-shaped Sb inclusions oriented toward the direction of solidification are present in the InSb matrix. The initial and final temperatures as well as the enthalpy of melting have been determined for this composite. The observed anisotropy of the temperature dependence of electrical conductivity of the composite has been attributed to the short-circuiting effect induced by inclusions.

Keywords: eutectic composite, structure, X-ray diffraction, scanning electron microscopy, thermal and electrical conductivity.

<https://doi.org/10.15407/spqeo29.01.040>

PACS 07.20.Fw, 61.05.cp, 68.37.Hk, 78.30.Fs, 81.30.-t

Manuscript received 08.08.25; revised version received 11.02.26; accepted for publication 18.03.26; published online 25.03.26.

1. Introduction

One of the main features of eutectic composites containing InSb, GaSb and 3d-transition components is anisotropy of the kinetic coefficients based on metal needle direction [1–4]. The composites exhibit nonhomogeneous semiconductor behavior due to the parallel arrangement of metal needles with respect to the direction of crystallization. One example of such composites that deserve particular attention are InSb–Sb composites. This work focuses on synthesis and structural characterization of InSb–Sb eutectic composites.

With their steady composition and characteristics, diluted semiconductor materials based on A³B⁵ compounds and 3d-metals eutectic composites show promise as materials for spintronic devices. The anisotropy in the kinetic coefficients based on the direction of metal needles is one of the primary characteristics of eutectic composites consisting of InAs, InSb, GaSb, GaSe and 3d-transition elements. An important III-V semiconductor InSb has attracted great attention due to its unique physical properties. For example, InSb is a good electrical conductor because of its narrow bandgap and high charge carrier mobility. However, its high lattice thermal conductivity restricts its applicability for thermoelectric applications. The interest to this material has grown recently because of its fascinating thermoelectric (TE) behavior, which enables heat to be directly transformed into electrical power [3–8].

A significant attention has been given to suitability of unidirectionally solidified eutectic alloys to use them as high temperature materials. One of the most important requirements is for this is maintenance of the aligned structure of the composite during service. Much effort has been put to determine the high temperature stability of aligned composites [8–12], *i.e.* the effect of aging of eutectic alloys at high temperatures on composite alignment during coarsening.

2. Experimental results and discussion

The ingots were grown in a Bridgman furnace at varying growth rates. Metallographic examination revealed an eutectic structure with continuous rods of Sb in an InSb matrix, always oriented in the growth direction. The undercooling behavior of antimony and indium antimonide phases was investigated using high-purity antimony (99.999%).

The InSb component was evaluated, and a semiconductor grade material with a nominal purity level of 99.999% was chosen. The eutectic in an InSb–Sb system is close to 69.5 mol.% of Sb. In order to construct the target, we first developed the eutectic composition using the Bridgman method. This composition consisted of Sb inclusions and an InSb single crystalline matrix. The InSb–Sb eutectic specimens were made from ultrapure Sb (99.999%) and In (99.999%). The metals were taken in quantities corresponding to the InSb–Sb

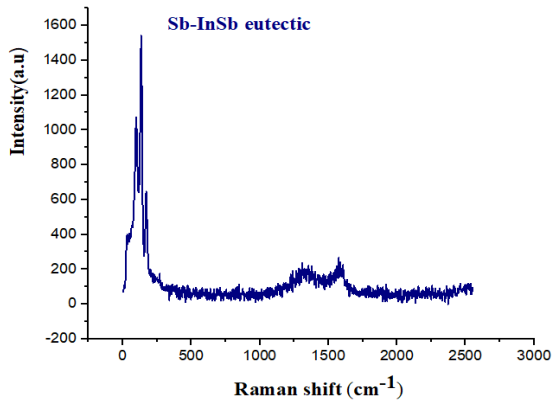


Fig. 1. Raman spectrum of a Sb–InSb eutectic composite.

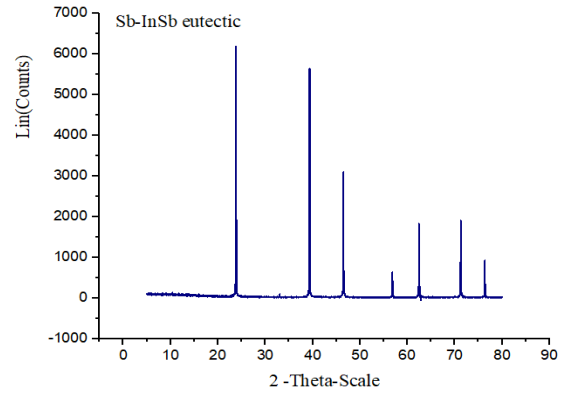


Fig. 2. XRD patterns of InSb–Sb eutectic systems.

eutectic composition and placed in a quartz tube that was vacuum-sealed. The weight percentage of this composition [3] was 30.5 for InSb and 69.5 for Sb. After melting, the samples were moved from the hot zone to the lower temperature zone to solidify at different rates. The InSb–Sb eutectic was used to illustrate how interface demarcation can be applied to investigate (directed) solidification of multiphase systems.

Raman analysis is an important method to study atomic interactions in semiconductors and dynamics of crystal lattice [3]. The Raman spectra of the InSb–Sb composites characterize only the Sb–Sb bonds (Fig. 1).

Fig. 2 shows the diffraction patterns of the InSb–Sb eutectic composite. X-ray phase analysis shows that the intense peaks corresponding to (111), (220), (311), (400), (311), (422) and (511) Müller indices are related to the matrix – InSb compound. The weak lines corresponding to the crystallographic parameters $a = 4.121$, $c = 5.467$ and $c/a = 1.327$ for the compound and the values of angles of 24° , 29° , 42° , 49° and 76° are related to Sb [11]. Sharp peaks in the diffractogram indicate the composite perfection.

The structure of the InSb–Sb eutectic system was examined by field-emission scanning electron microscopy (FESEM) and X-ray spectrography (Fig. 3). SEM and EDX analyses indicated that the obtained eutectics were two-phase systems. The data of the diffraction

patterns for Sb and InSb compounds are also displayed in this picture. The length of the metal rods ($1\text{--}1.8\ \mu\text{m}$ in diameter) in the InSb–Sb composite is $10\text{--}50\ \mu\text{m}$. As can be seen from Fig. 3, the metal rods are evenly distributed within the matrix in the direction of crystallization.

The eutectic InSb–Sb microstructure is highly sensitive to growth conditions during solidification. Directional solidification studies show that the rod morphology is stable. However, no extension to undercooled melt conditions has been done. The extent and shape of the coupled growth region remain unclear. The study evaluated undercooling and crystallization behavior of Sb and InSb, examining an eutectic mixture, exploring factors influencing undercooling and characterizing solidification microstructures. The droplet emulsion technique increases undercooling potential for pure Sb, InSb and InSb–Sb alloys by dividing the bulk ingot into droplets 10 to $150\ \mu\text{m}$ in size thus allowing for greater undercooling.

Higher cooling rates extend the metastable liquid state to lower temperatures, with droplet surface coating determining undercooling extent during solidification. A morphological transition from a rod to a lamellar structure occurs due to a change in the heat flow conditions. The thermal anisotropy of Sb encourages a change in the growth orientation, causing alignment of high conductivity planes and destroying the low energy orientation relationship between Sb rods and InSb matrix.

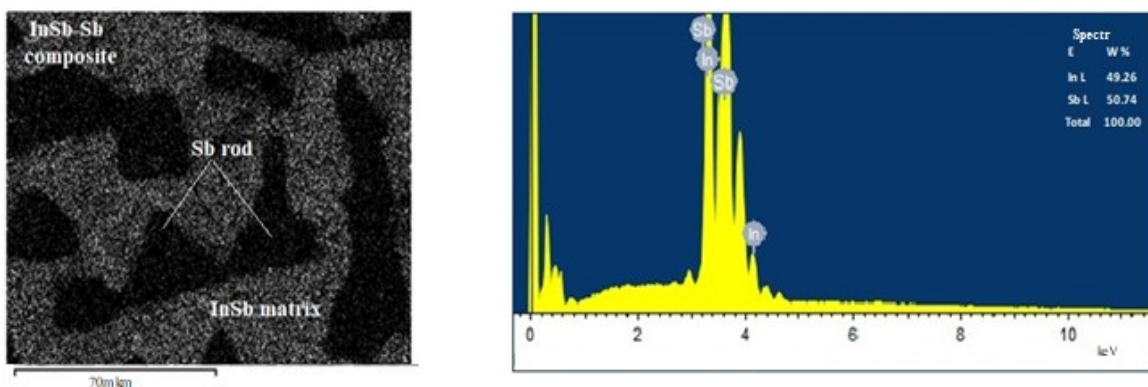


Fig. 3. X-ray spectra of Sb–InSb eutectic composite obtained from the rods and matrix phases along the lateral directions of the specimens using the scanning electron microscopy – energy dispersive X-ray spectroscopy method.

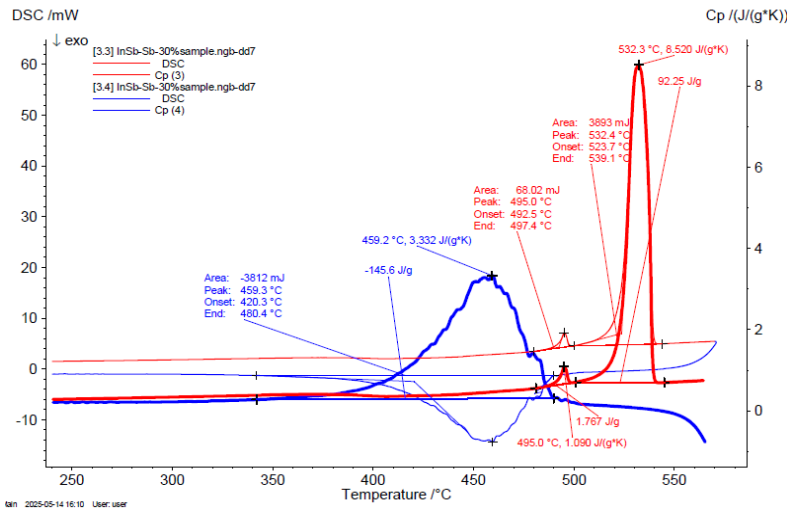


Fig. 4. DSC analysis results for the InSb–Sb eutectic composite.

The microstructures of the InSb–Sb eutectic composites are illustrated in Fig. 3, which shows both longitudinal and transverse sections obtained at various solidification rates. The rods were about 50 to 100 μm in length and about 4 to 20 μm in diameter. These dimensions decreased at increasing the solidification rate. The rod-like Sb appeared triangular in transverse cross-section.

This study shows that the eutectic crystallization process can be used to create two-phase materials with a well-known chemical composition and a highly organized structural layout. The two phases begin to crystallize simultaneously when an InSb–Sb melt of eutectic composition is cooled below the eutectic temperature. During this process, each InSb crystallite is surrounded by a Sb-rich undercooled liquid layer, and each Sb crystallite is surrounded by an InSb-rich liquid layer. Steady-state crystallization, at which InSb and Sb crystallites of constant dimensions grow parallel to each other at the same rate until the entire liquid solidifies, can be maintained provided that the excess Sb in front of the InSb crystallites can diffuse to the Sb crystallites. Such a steady-state crystallization process has been obtained by directional solidification of InSb–Sb eutectic melts using a sharp temperature gradient.

The eutectic spacing, a measure of the fraction solidified within a droplet, indicates growth conditions during recalescence. It increases after nucleation until reaching a transition zone, where droplet solidification is nonadiabatic due to nonzero undercooling.

Knowing the precise composition of an InSb ingot can facilitate examination of the pure constituent, eliminating potential primary phase formation effects. Melt spinning or rapid heat extraction from the eutectic alloy should be used to assess the impact of exceeding the theoretical growth velocity limit for coupled growth.

The In–Sb binary system undergoes a eutectic reaction, resulting in a two-phase mixture of InSb and Sb. The resulting microstructure, consisting of InSb intermetallic inclusions embedded in a Sb matrix, provides

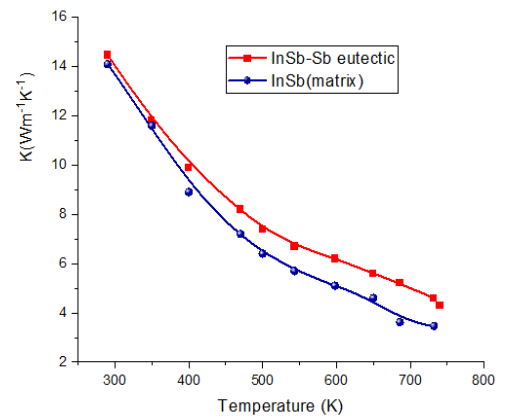


Fig. 5. Thermal conductivity of InSb and InSb–Sb eutectic composite.

numerous phase boundaries that act as effective barriers to phonon transport. This suppression of phonon propagation reduces thermal conductivity, highlighting the potential of the InSb–Sb eutectic system for thermoelectric and other thermal management applications.

The study successfully improved the thermoelectric performance of InSb-based alloys by optimizing eutectic composition, achieving an unprecedented high thermoelectric figure of merit (ZT) of 1.3 at 450 $^{\circ}\text{C}$.

Fig. 3 shows the results of the differential scanning calorimetry (DSC) analysis, providing insight into the thermal stability of the sample. The first endothermic peak at 459.2 $^{\circ}\text{C}$, corresponding to a heat flow of 92.25 J/g and a specific heat capacity (C_p) of 8.52 J/g·K, points to a solid-state reaction or partial phase transformation. This indicates that the sample undergoes structural rearrangements prior to melting, which may influence its microstructure and physical properties. The second, more pronounced endothermic peak at 532.3 $^{\circ}\text{C}$, corresponding to a heat flow of 68.02 J/g and C_p of 1.09 J/g·K, corresponds to melting of the InSb–Sb eutectic phase. The sharpness and well-defined nature of this peak indicate a uniform eutectic composition and good homogeneity of the sample. These observations are consistent with literature values for the InSb–Sb eutectic system, confirming successful formation of the intended phase. The thermal behavior observed here also implies that the sample has a well-ordered microstructure, as broad or multiple peaks would indicate compositional heterogeneity or presence of intermediate phases. Understanding these phase transitions, along with obtaining the associated heat capacities, is critical for optimizing

Peak	DSC area, J/g	C_p , J/g·K	
459.2 $^{\circ}\text{C}$	92.25	8.520	endothermic
532.3 $^{\circ}\text{C}$	68.02	1.09	endothermic

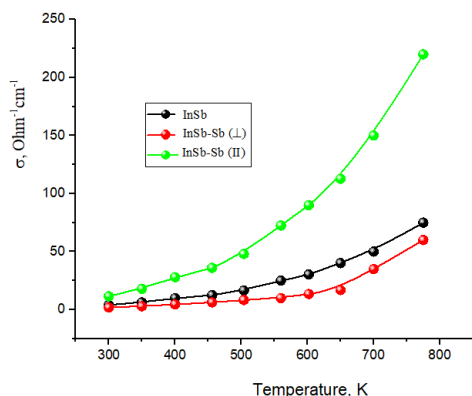


Fig. 6. Temperature dependence of electric conductivity of InSb and Sb–InSb composite.

processing conditions, as the solid-state transformations and eutectic melting behavior directly affect material performance, especially in applications requiring precise thermal management. Overall, the DSC results demonstrate that the sample exhibits predictable and well-defined thermal transitions, reflecting both compositional uniformity and stable phase formation.

Temperature dependences of thermal conductivity $K(T)$ of InSb and InSb–Sb eutectic composite are shown in Fig. 5. The thermal conductivity of the eutectic alloys shows a noticeable drop most likely caused by interaction of phonons with phase boundaries. An eutectics having a lower melting point than its components can reduce thermal conductivity and enhance ZT by introducing a suitable amount into the compound [13–19].

Eutectic systems with melting temperatures lower than those of their individual constituents, can be incorporated in controlled amounts to reduce thermal conductivity and thereby improve the thermoelectric figure of merit. During solidification of an eutectic melt, two distinct crystalline phases (such as InSb and Sb) nucleate and grow concurrently, giving rise to a complex microstructure with a high density of interphase boundaries. These interfaces act as efficient phonon-scattering centers, significantly impeding heat-carrying phonons and leading to a pronounced reduction in lattice thermal conductivity. The resulting multiphase, heterogeneous microstructure effectively disrupts phonon transport, which is a key mechanism for enhancing ZT.

Excess Sb forms an eutectic-included composite microstructure due to strong phonon scattering at the solid-liquid interfaces and enhanced ZT upon melting.

Fig. 6 shows temperature dependences of electrical conductivity $\sigma(T)$ at various mutual directions of current (I), magnetic field (B) and crystallization.

The presence of regular metal crystalline inclusions in the semiconductor matrix causes anisotropy in the temperature dependence of the kinetic coefficients [14–19]. Electrical conductivity rises in the $I||x$ direction due to short-circuiting by needle-shaped metallic inclusions, and greatly differs from $\sigma(T)$ in the $I \perp x$ direction. As the temperature rises, the coefficient of conductivity anisotropy decreases reaching $\sigma_{||}/\sigma_{\perp} = 3$.

3. Conclusions

Directional solidification produced a well-aligned InSb–Sb eutectic microstructure, featuring continuous, needle-like Sb inclusions oriented along the growth direction. Differential scanning calorimetry revealed high thermal stability, a sharp eutectic melting peak at 532.3 °C, indicating compositional uniformity. The anisotropic, needle-shaped Sb inclusions induce pronounced electrical conductivity anisotropy, with enhanced conductivity parallel to the growth direction that decreases with increasing temperature. Raman spectroscopy indicated that lattice dynamics are dominated by Sb–Sb bonding, while dense InSb–Sb interfaces effectively suppress phonon transport. This combination results in reduced thermal conductivity and enhanced thermoelectric performance.

References

1. Kazimov M.V., Ibragimov G.B. Fabrication and performance characterization of Sb_2Se_3 -GaSe eutectic systems. *SPQEO*. 2024. **27**, No 2. P. 184–188. <https://doi.org/10.15407/spqeo27.02.184>.
2. Kazimov M.V. Synthesis and structural analysis of InSb–CrSb, InSb–Sb, GaSb–CrSb eutectic composites. *J. Optoelectron. Biomed. Mater.* 2020. **12**. P. 67–72.
3. Kazimov M.V., Ibragimov G.B., Isakov G.I., Ibragimov B.G. Physical-chemical properties of InSb+ Mg_3Sb_2 eutectic systems: Synthesis, characterization, and applications. *J. Optoelectron. Biomed. Mater.* 2022. **14**, No 4. P. 187–190. <https://doi.org/10.15251/JOBM.2022.144.187>.
4. Kazimov M.V., Arasly D.H., Rahimov R.N. *et al.* Magnetic and electrical properties of GaSb–CrSb eutectic system. *J. Non-Oxide Glasses*. 2020. **12**. P. 7–11. <https://doi.org/10.13140/RG.2.2.19921.68965>.
5. Graves J.A. *Undercooling and Solidification Behavior in the InSb-Sb System*, NASA CR-175013, September 1985. P. 216. <https://ntrs.nasa.gov/citations/19860004885>.
6. Ibragimov G.B. Free-carrier absorption in quantum wires for boundary roughness scattering. *J. Phys. Condens. Matter*. 2003. **15**, No 9. P. 1427–1435. <https://doi.org/10.1088/0953-8984/15/9/306>.
7. Joya M.R., Pizania P.S., Jasinevicius R.G. Raman scattering investigation on structural and chemical disorder generated by laser ablation and mechanical microindentations of InSb single crystal. *J. Appl. Phys.* 2006. **100**. P. 053518. <https://doi.org/10.1063/1.2345052>.
8. Abaker M., Ahmed N.E., Saad A. *et al.* Thermoelectric properties of Ga-doped InSb alloys. *Vacuum*. 2024. **219**, Part A. P. 112761. <https://doi.org/10.1016/j.vacuum.2023.112761>.
9. Kazimov M.V., Ibragimov G.B. X ray analysis of InAs–CrAs eutectic systems. *ARCENG*. 2023. **3**. P. 32–35. <https://doi.org/10.5281/zenodo.8106289>.
10. Alekberov R.I., Mekhtiyeva S.I., Mammadov S.M. *et al.* The influence of a hydrocarbon environment with aliphatic and cyclic chain structures on the volt-ampere characteristic of the Al- $Ge_{33}As_{17}S_{35}Se_{15}$ -Te

- sandwich structure. *Chalcogenide Lett.* 2024. **21**. P. 927–931. <https://doi.org/10.15251/CL.2024.2111.927>.
11. Ye Q., Scheffler R., Kumari J., Leverenz R. Growth and characterization of single crystalline InSb nanowires for thermoelectric applications. *NSTI Nanotech.* 2007. 1. P. 237–240.
 12. Berus T., Goc J., Nowak M. *et al.* Preparation and electrical properties of InSb thin films heavily doped with tellurium, selenium and sulphur. *Thin Solid Films.* 1984. **111**, Issue 4. P. 351–366. [https://doi.org/10.1016/0040-6090\(84\)90327-4](https://doi.org/10.1016/0040-6090(84)90327-4).
 13. Okimura H., Koizumi Y., Kaida S. Electrical properties of *p*-type InSb thin films prepared by coevaporation with excess antimony. *Thin Solid Films.* 1995. **254**, Issues 1–2. P. 169–174. [https://doi.org/10.1016/0040-6090\(94\)06233-B](https://doi.org/10.1016/0040-6090(94)06233-B).
 14. Cai X., Wei J. Temperature dependence of the thermal properties of InSb materials used in data storage. *J. Appl. Phys.* 2013. **114**. P. 083507. <https://doi.org/10.1063/1.4819224>.
 15. Rahimov R.N., Kazimov M.V., Arasly D.H. *et al.* Features of thermal and electrical properties of GaSb–CrSb eutectic composite. *J. Ovonic Res.* 2017. **13**, No 3. P. 113–118.
 16. Balagurov B.Ya., Vinogradov G.A., Thermal conductivity of composites with needle-shaped inclusions. *Composites, Pt A.* 2006. **37**. P. 1805–1814. <https://doi.org/10.1016/j.compositesa.2005.08.019>.
 17. Tagiyev M.M., Aliyeva Kh.F. Anisotropic thermoelectrics based on an extruded sample of Bi_{0.85}Sb_{0.15} solid solution doped with tellurium. *UNEC J. Eng. Appl. Sci.* 2025. **5**, No 1. P. 70–82. <https://doi.org/10.61640/ujeas.2025.0508>.
 18. Huseynova A., Rzayev R., Hajiyeva F. Influence of electrothermopolarization process on the structure and properties of nanocomposites based on high-density polyethylene and HfO₂ nanoparticle. *J. Korean Phys. Soc.* 2024. **85**, No 1. P. 76–90. <https://doi.org/10.1007/s40042-024-01094-8>.
 19. Rahimli A., Huseynova A., Musayeva N. *et al.* Insights into dielectric and thermal properties of polystyrene-zinc oxide nanocomposites: A multifaceted characterization approach. *J. Thermoplast. Compos. Mater.* 2024. **38**, No 4. P. 1542–1556. <https://doi.org/10.1177/08927057241274265>.

Authors and CV



M.V. Kazimov, PhD, Associate Professor, Head of the “Nano and Active Composites” laboratory at the Institute of Physics of the Ministry of Science and Education of the Republic of Azerbaijan. The author is engaged in electric charge and heat transfer mechanisms in semiconductor- and metal-based eutectic composites. Authored over 50 publications and 2 textbooks. <https://orcid.org/0009-0002-4722-6149>



G.B. Ibragimov, DSc., Professor, Executive Director of the Institute of Physics of the Ministry of Science and Education of the Republic of Azerbaijan. Authored of 215 scientific works, 95 of which are included in the scientific databases Scopus and Web of Science. He is engaged in the study of optical phenomena and kinetic effects in semiconductors and low-dimensional systems. E-mail: guseyn_gb@mail.ru, <https://orcid.org/0009-0000-4439-9111>



B.G. Ibrahimov, PhD, Associate Professor, Leading Scientific Researcher at the laboratory “Transport Phenomena in Semiconductors and Semiconductor Nanostructures” of the Institute of Physics of the Ministry of Science and Education of the Republic of Azerbaijan. He is the author of 32 scientific works. He is engaged in the study of optical phenomena and kinetic effects in semiconductors and low-dimensional systems. <https://orcid.org/0009-0004-4990-3590>, e-mail: guseyn_gb@mail.ru

Authors' contributions

- Kazimov M.V.:** investigation, methodology, project administration, methodology, data curation, writing – original draft, writing – review & editing.
- Ibragimov G.B.:** investigation, formal analysis, supervision, conceptualization, validation, writing – original draft, writing – review & editing.
- Ibrahimov B.G.:** investigation, formal analysis, supervision, conceptualization, validation, writing – original draft.

Удосконалені евтектичні сплави Sb–InSb з адаптованими інтерфейсами для високої термоелектричної ефективності

M.V. Kazimov, G.B. Ibragimov, B.G. Ibrahimov

Анотація. Проаналізовано евтектичний композит Sb–InSb, виготовлений за методом Бріджмена з використанням структурного аналізу, диференціального скануючого аналізу, раманівського розсіювання та рентгенівської дифракції. Було показано, що в матриці InSb присутні голкоподібні включення Sb, орієнтовані в напрямку затвердіння. Для цього композиту було визначено початкову та кінцеву температури, а також ентальпію плавлення. Анізотропію у температурній залежності електропровідності композиту було пояснено ефектом закорочування, спричиненим включеннями.

Ключові слова: евтектичний композит, структура, дифракція рентгенівських променів, скануюча електронна мікроскопія, тепло- та електропровідність.